On the Performance Analysis of WPT-based Dual-Hop AF Relaying Networks in α-μ Fading

Galymzhan Nauryzbayev, *Member, IEEE,* Khaled M. Rabie, *Member, IEEE,*
Mohamed Abdallah, *Senior Member, IEEE*, and Bamidele Adebisi, *Senior Member, IEEE*

Abstract—In this paper, a two-hop amplify-and-forward relaying system, where an energy-constrained relay node entirely depends on the energy scavenged from the source signal, is investigated. This paper analyzes the performance of the EH protocols, namely, ideal relaying receiver (IRR), power-splitting relaying (PSR) and time-switching relaying (TSR), over independent but not identically distributed (i.n.i.d.) α-μ fading channels in terms of the ergodic capacity and ergodic outage probability (OP). We derive exact unified and closed-form analytical expressions for the performance metrics with the aforementioned protocols over i.n.i.d. α-μ channels. Three fading scenarios, such as Weibull, Nakagami-m and Rayleigh channels, are investigated. Provided simulation and numerical results validate our analysis. It is demonstrated that the optimal EH time-switching and power-splitting factors of the corresponding TSR and PSR protocols are critical in achieving the best system performance. Finally, we analyzed the impact of the fading parameters α and μ on the achievable ergodic OP.

Index Terms—Wireless power transfer (WPT), α-μ fading, amplify-and-forward (AF) relaying, ergodic capacity (EC), energy-harvesting (EH), outage probability (OP).

I. INTRODUCTION

WIRELESS power transfer (WPT) has recently drawn considerable attention from both academia and industry as a promising technology enabling the life-time prolongation of wireless battery-powered devices [1]–[3]. The exploitation of radio-frequency (RF) signals for simultaneous energy and information delivery, best known as simultaneous wireless information and power transfer (SWIPT), is believed to be one of the main efficient techniques for wireless energy-harvesting (EH). Some examples of the most well-known SWIPT architectures in the literature include time-switching (TS), power-splitting (PS) and ideal relaying protocols [4]–[9].

Recently, the performance of SWIPT relaying systems has been broadly investigated, where the relay nodes scavenge energy from the received RF signals and then utilize it to forward the desired information to their intended destinations. For example, in [6], the performance of the dual-hop amplify-and-forward (AF) relaying system over Rayleigh channels was analyzed. This work studied three EH relaying protocols: ideal relaying receiver (IRR), power-splitting relaying (PSR) and time-switching relaying (TSR). Moreover, the outage probability (OP) of dual-hop decode-and-forward (DF) underlay cooperative cognitive networks with interference alignment was evaluated in [10] implementing the PSR and TSR relaying protocols over Rayleigh fading. Additionally, [8] derived exact numerical expressions of the achievable throughput and ergodic capacity (EC) of the PSR- and TSR-based DF relaying

systems over Rayleigh fading. Moreover, the authors in [9], [11], [12] studied the OP in dual-hop DF and AF relaying networks fading channels considering both half-duplex (HD) and full-duplex (FD) with several EH protocols. In addition, an IRR protocol with EH constraints in AF relaying systems was considered in [6], [7] and [13]. The transmission rate and outage performance for FD DF relaying networks were investigated in [14] and [15], respectively. Another aspects such as energy efficiency and security issues in a WPT-enabled FD-DF relaying network were studied in [16]. The authors in [17] and [18] investigated the secrecy rate and energy efficiency in wireless powered massive multiple-input multiple-output (MIMO) networks, respectively. In addition, the authors in [19] analyzed the degrading effect such as inter-relay interference in the WPT-enabled MIMO virtual FD relaying scheme. Recently, the authors in [20]–[22] considered a non-orthogonal multiple access (NOMA) approach in wireless powered relaying systems. For instance, the work in [20] and [21] investigated the outage and data rate performance of PS-based downlink cooperative SWIPT NOMA systems. Furthermore, the authors in [22] studied the outage performance and energy efficiency of WPT-based AF NOMA relaying networks over Nakagami-m fading channels.

Very recently, the author in [23] provided a closed-form expression for the OP in wireless powered DF-based systems over α-μ fading channels. However, to the best of the authors' knowledge, wireless powered AF relaying systems over independent and not necessarily identically distributed (i.n.i.d.) α-μ fading channels have not analyzed in the literature. Therefore, we dedicate this paper to derive new closed-form expressions for the ergodic OP and the EC over i.n.i.d. α-μ fading channels in a dual-hop AF relaying network. It is worthwhile mentioning that small-scale fading channels, such as Weibull, Nakagami-m, etc. [24], can be described by the generalized α-μ statistical model.

The obtained expressions are unified meaning that they represent three different EH protocols, such as IRR, PSR and TSR, and various fading channels which are obtainable from the α-μ statistical model. The derived exact analytical expressions provide insights into the operation of the protocols under different parameters comprising various distinct scenarios of the α-μ model, namely, Weibull, Nakagami-m and Rayleigh fading channels. Throughout this work, Monte Carlo simulations validate our theoretical results. Results reveal that the achievable EC of the TSR and PSR protocols can be maximized by optimizing the EH PS and TS factors. It is also shown that the optimized PSR protocol always outperforms the
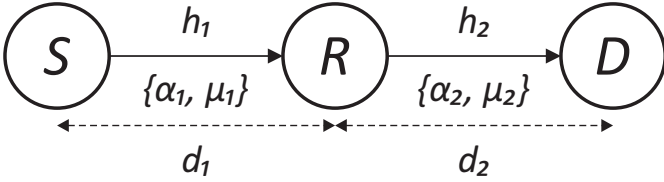
Fig. 1. Diagram of the considered two-hop AF relaying system.

Fig. 2. Time frame structures for different EH protocols.

optimized TSR one while the best performance is achieved in the IRR protocol. The good agreement between the simulation and analytical results clearly indicates the correctness of the analysis. Finally, we analyzed the impact of the fading parameters on the ergodic OP for the IRR protocol as a function of α and μ, i.e. the ergodic OP improves as the values of α and/or μ increase.

The remainder of this paper is organized as follows. The system model and the two performance metrics adopted in this paper are described in Section II. New closed-form analytical expressions for the EC and ergodic OP are derived for TRR, PSR and IRR protocols over i.n.i.d. α-μ fading channels in Sections III, IV and V, respectively. Analytical and simulated results are provided and discussed in Section VI. Finally, Section VII concludes the paper.

II. SYSTEM AND CHANNEL MODEL

The system model considered in this study consists of three nodes: a source (S), a relay (R) and a destination (D). The overall S-to-D communication is realized over two time periods as presented in Fig. 1. The first phase is dedicated for the EH and S-to-R transmission while the second phase is used for the R-to-D communication when R amplifies and then forwards the received signal to D. During the first phase, R scavenges energy from the signal sent by S with power P_S. For the sake of completeness, we next briefly review the operation of the three considered EH protocols given in Fig. 2; more details can be found in [6].

Fig. 1 depicts a two-hop AF relaying system, where S sends data to D via the energy-constrained AF-based R (i.e., powered by the harvested power only). It is assumed that no direct link exists between S and D and each nodes operates in the HD mode and is deployed with a single-antenna. Moreover, the amount of power required by R for data processing is assumed to be negligible. h_1 and h_2 represent the S-to-R and R-to-D links subject to quasi-static i.n.i.d. α-μ fading with corresponding distances d_1 and d_2, respectively. m_1 and m_2 denote the corresponding path-loss exponents. Note that the channel coefficients vary independently from one transmission time block T to another while remaining constant during one T. Then, a certain hop i is characterized by the corresponding probability density function (PDF) defined as [25]

$$f_{h_i}(r) = \frac{\alpha_i \mu_i^{\mu_i} r^{\alpha_i \mu_i - 1}}{\hat{r}^{\alpha_i \mu_i} \Gamma(\mu_i)} \exp\left(-\frac{\mu_i}{\hat{r}^{\alpha_i}} r^{\alpha_i}\right), \quad (1)$$

where $\hat{r}$ stands for a α_i−root mean value given by $\hat{r} = \sqrt[\alpha_i]{\mathbb{E}[r^{\alpha_i}]}$, $\alpha_i > 0$ is an arbitrary parameter, $\mathbb{E}[\cdot]$ is the expectation operator and $\Gamma(s) = \int_0^\infty t^{s-1} e^{-t} dt$ denotes the
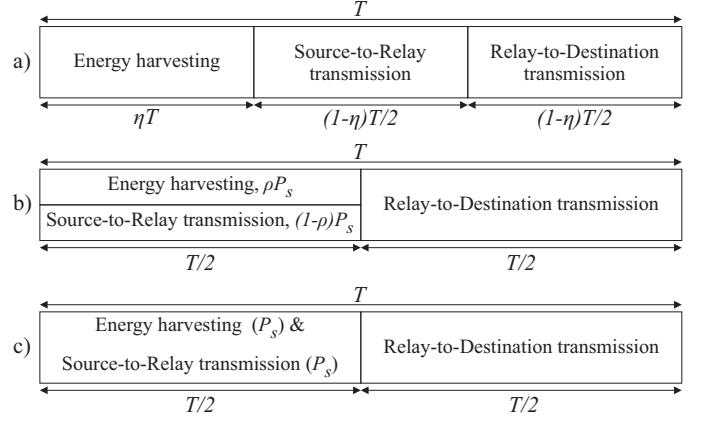
Gamma function [26]. Also, $\mu_i = \frac{\mathbb{E}[r^{\alpha_i}]}{(\mathbb{E}[r^{2\alpha_i}] - \mathbb{E}^2[r^{\alpha_i}])} \geq \frac{1}{2}$ indicates the inverse of normalized variance of r^{α_i}.

It is worthwhile noting that the α-μ distribution represents the most suitable statistical model describing small-scale fading channels such as Weibull (α is the fading parameter with $\mu = 1$), Nakagami−m (μ is the fading parameter with $\alpha = 2$), Rayleigh ($\alpha = 2$, $\mu = 1$), etc. [24].

A. Ergodic Capacity

The instantaneous capacity of the end-to-end signal-to-noise ratio (SNR) is defined as

$$C_D = \frac{\phi}{2} \log_2(1 + \gamma_D), \quad (2)$$

where γ_D indicates the SNR at D and the factor $\frac{1}{2}$ implies that two time slots (TSs) are required for S-to-D communication. Moreover, $\phi = (1-\eta)$ defines the capacity of the TSR protocol while $\phi = 1$ determines the capacity achievable under the PRS and IRR protocols. Using (2), the EC can be defined as

$$\mathbb{E}[C_D] = \frac{\phi}{2} \mathbb{E}[\log_2(1 + \gamma_D)]. \quad (3)$$

B. Outage Probability

Using (2), the ergodic OP can be expressed as

$$P_{\text{out}} = \Pr(C_D < \mathcal{R}) = \Pr\left(\gamma_D < 2^{\frac{2\mathcal{R}}{\phi}} - 1\right), \quad (4)$$

where $\mathcal{R}$ indicates the minimum required rate.

III. PERFORMANCE ANALYSIS OF THE TSR-BASED SYSTEM

The given transmission time block T needed for S-to-D communication is formed by three consecutive TSs. The first TS is dedicated for EH while the remaining two TSs are designated to support the S-to-R and R-to-D data transmissions, i.e., ηT, $(1 - \eta)T/2$, and $(1 - \eta)T/2$, respectively, where $0 \leq \eta \leq 1$ denotes the EH time factor as shown in Fig. 2(a).

The received signal at R can be expressed as [9]

$$y_R(t) = \sqrt{\frac{P_S}{d_1^{m_1}}} h_1 s(t) + n_a(t), \quad (5)$$

where P_S, $n_a(t)$, with variance σ_a^2, and $s(t)$, with $\mathbb{E}\left[|s(t)|^2\right] = 1$, stand for the source transmit power, noise term and information signal at R, respectively. Therefore, R scavenge the energy defined as

$$E_H^{TSR} = \theta\eta T\left(\frac{P_S}{d_1^{m_1}}h_1^2 + \sigma_a^2\right), \tag{6}$$

where $0 < \theta \leq 1$ is the EH conversion efficiency mainly affected by the circuitry. With this in mind, after base-band processing, R amplifies the signal as

$$s_R(t) = \sqrt{\frac{P_R P_S}{d_1^{m_1}}}Gh_1 s(t) + \sqrt{P_R}Gn_R(t), \tag{7}$$

where P_R denotes the relay transmit power, $G = 1/\sqrt{\frac{P_S}{d_1^{m_1}}h_1^2 + \sigma_R^2}$ is the relay gain and $n_R(t) = n_a(t) + n_c(t)$ denotes the overall noise at R with variance $\sigma_R^2 = \sigma_a^2 + \sigma_c^2$, where $n_c(t)$ stands for the noise term caused by the information receiver. Hence, D receives the signal as

$$y_D(t) = \sqrt{\frac{P_R}{d_2^{m_2}}}Gh_2\left(\sqrt{\frac{P_S}{d_1^{m_1}}}h_1 s(t) + n_R(t)\right) + n_D(t), \tag{8}$$

where $n_D(t)$, with variance σ_D^2, indicates the noise at D. The relay transmit power relates to the harvested energy as $P_R = E_H^{TSR}/\left((1-\eta)T/2\right)$ and can be rewritten using (6) as

$$P_R = \frac{2\theta\eta}{1-\eta}\left(\frac{P_S}{d_1^{m_1}}h_1^2 + \sigma_a^2\right). \tag{9}$$

Substituting (9) into (8) and after some algebraic manipulations, the SNR at D can be written as

$$\gamma_D = \frac{2\theta\eta P_S h_1^2 h_2^2}{2\theta\eta h_2^2 d_1^{m_1}\sigma_R^2 + (1-\eta)d_1^{m_1}d_2^{m_2}\sigma_D^2}. \tag{10}$$

A. Ergodic Capacity

Now, by defining $a_1 = 2\theta\eta P_S$, $a_2 = (1-\eta)d_1^{m_1}d_2^{m_2}\sigma_D^2$, $a_3 = 2\theta\eta d_1^{m_1}\sigma_R^2$, $\mathcal{A} = a_1 X$, and $\mathcal{B} = a_2\bar{Y}$, where $X = h_1^2$ and $\bar{Y} = h_2^{-2}$, the SNR γ_D can be written as

$$\gamma_D = \frac{\mathcal{A}}{\mathcal{B} + a_3}. \tag{11}$$

Using (3) and (11), we can express the EC as

$$\mathbb{E}\left[C_D\right] = \frac{1-\eta}{2}\mathbb{E}\left[\log_2\left(1 + \frac{\mathcal{A}}{\mathcal{B} + a_3}\right)\right]. \tag{12}$$

The term $(1-\eta)$ means that the information is communicated only within $(1-\eta)T$ while the rest is utilized for EH purposes.

We use the lemma to facilitate the EC analysis [32] as

$$\mathbb{E}\left[\ln\left(1 + \frac{u}{v}\right)\right] = \int_0^\infty \frac{1}{s}\left(\Phi_v(s) - \Phi_{v,u}(s)\right)\mathrm{d}s, \ \forall \ u, v > 0, \tag{13}$$

where the random variable (RV) v is characterized by its moment generating function (MGF) $\Phi_v(s)$. If v and u are independent, then $\Phi_{v,u}(s)$ can be defined as $\Phi_{v,u} = \Phi_v(s)\Phi_u(s)$. Therefore, using (13), the EC at D can be evaluated as

$$\mathbb{E}\left[C_D\right] = \frac{1-\eta}{2\ln(2)}\int_0^\infty \frac{1}{s}\left(1 - \Phi_{\mathcal{A}}(s)\right)\Phi_{\mathcal{B}+a_3}(s)\mathrm{d}s, \tag{14}$$

where $\Phi_{\mathcal{A}}(s) = \Phi_X(a_1 s)$ and $\Phi_{\mathcal{B}+a_3}(s) = \Phi_{\bar{Y}}(a_2 s)\exp\left(-a_3 s\right)$ stand for the MGFs of $\mathcal{A}$ and $\mathcal{B} + a_3$, respectively. Since $X = h_1^2$ and $\bar{Y} = h_2^{-2}$ follow the α-μ statistical model, we modify the PDF in (1) applying the "change of variable" method [7]. Therefore, we rewrite the corresponding PDFs in the following form

$$f_X(r) = \frac{\alpha_1\lambda_1^{\mu_1}r^{\frac{\alpha_1\mu_1}{2}-1}}{2\Gamma(\mu_1)}\exp\left(-\lambda_1 r^{\frac{\alpha_1}{2}}\right), \tag{15}$$

$$f_{\bar{Y}}(r) = \frac{\alpha_2\lambda_2^{\mu_2}r^{-\frac{\alpha_2\mu_2}{2}-1}}{2\Gamma(\mu_2)}\exp\left(-\lambda_2 r^{-\frac{\alpha_2}{2}}\right), \tag{16}$$

where $\lambda_1 = \frac{\mu_1}{\hat{r}^{\frac{\alpha_1}{2}}}$ and $\lambda_2 = \frac{\mu_2}{\hat{r}^{\frac{\alpha_2}{2}}}$. The MGF defined as $\Phi(s) = \int_0^\infty \exp\left(-sr\right)f(r)\mathrm{d}r$ will be utilized in the EC analysis. The corresponding MGFs of these PDFs can be presented as

$$\Phi_X = \frac{\alpha_1\lambda_1^{\mu_1}}{2\Gamma(\mu_1)}\int_0^\infty r^{\frac{\alpha_1\mu_1}{2}-1}e^{-sr}e^{-\lambda_1 r^{\frac{\alpha_1}{2}}}\mathrm{d}r, \tag{17}$$

$$\Phi_{\bar{Y}} = \frac{\alpha_2\lambda_2^{\mu_2}}{2\Gamma(\mu_2)}\int_0^\infty r^{-\frac{\alpha_2\mu_2}{2}-1}e^{-sr}e^{-\lambda_2 r^{-\frac{\alpha_2}{2}}}\mathrm{d}r. \tag{18}$$

Using [27, Eq. (8.4.3.1)], [27, Eq. (2.24.1.1) and (8.2.2.14)], the MGFs of X and $\bar{Y}$ can be expressed in terms of Meijer's $G-$functions as in (19) and (20), respectively, shown at the top of the next page. l_i and k_i denote the co-prime numbers, with $l_i/k_i = \alpha_i/2$ and $\Delta\left(\beta, \iota\right) = \left\{\frac{\iota}{\beta}, \frac{\iota+1}{\beta}, \ldots, \frac{\iota+\beta-1}{\beta}\right\}$. It is worthwhile mentioning that a similar derivation approach will be used for the other EH protocols. Moreover, $\Phi_{\mathcal{A}}$ and $\Phi_{\mathcal{B}+a_3}$ can be obtained as in (21) and (22), shown at the top of the next page.

Finally, using [28, Eq. (6.2.8)] and [29, Eq. (2.3)], the end-to-end EC of the TSR-based system can be expressed as in (23), shown at the top of the next page, where $\kappa = \frac{2\theta\eta}{(1-\eta)}$, $H_{p,q}^{m,n}\left(\cdot\right)$ denotes the Fox's H-function, defined by [30, Eq. (1.2)], and $H_{p_1,q_1:p_2,q_2:p_3,q_3}^{m_1,n_1:m_2,n_2:m_3,n_3}\left(\cdot\right)$ denotes the extended generalized bivariate Fox's H-function (EGBFHF), defined by [30, Eq. (2.57)]. $A = \left\{1 - \Delta\left(k_1, 0\right)\right\}$, $B = \left\{1 - \Delta\left(l_1, 1 - \frac{\alpha_1\mu_1}{2}\right)\right\}$ and $C = \left\{\Delta\left(k_2, 0\right), \Delta\left(l_2, -\frac{\alpha_2\mu_2}{2}\right)\right\}$. Note that (k_i, l_i) are co-prime numbers; α_i is the fading parameter defined as $\alpha_i = \frac{2l_i}{k_i}$ for $i = \{1, 2\}$ and $k_i, l_i = 1, 2, 3, \ldots$

B. Ergodic Outage Probability

The SNR γ_D at D given in (10) can be rewritten as

$$\gamma_D = \frac{\beta_1 XY}{\beta_2 Y + \beta_3}, \tag{24}$$

where $\beta_1 = 2\eta\theta P_S$, $\beta_2 = 2\eta\theta d_1^m\sigma_R^2$, $\beta_3 = (1-\eta)d_1^m d_2^m\sigma_D^2$, $X = h_1^2$ and $Y = h_2^2$.

We define the PDF of Y using [7] as

$$f_Y(r) = \frac{\alpha_2\lambda_2^{\mu_2}r^{\frac{\alpha_2\mu_2}{2}-1}}{2\Gamma(\mu_2)}\exp\left(-\lambda_2 r^{\frac{\alpha_2}{2}}\right). \tag{25}$$

The ergodic OP can be expressed, using (2) and (24), as

$$P_{\text{out}} = \Pr\left(\frac{\beta_1 XY}{\beta_2 Y + \beta_3} < \gamma_{th}\right)$$

$$= \Pr\left(Y < \frac{\beta_3\gamma_{th}}{\beta_1 X - \beta_2\gamma_{th}}\right), \tag{26}$$

$$\Phi_X(s) = \frac{\alpha_1 \lambda_1^{\mu_1} k_1^{\frac{1}{2}} l_1^{\frac{\alpha_1\mu_1-1}{2}} s^{-\frac{\alpha_1\mu_1}{2}}}{2\Gamma(\mu_1)(2\pi)^{\frac{l_1+k_1-2}{2}}} G_{k_1,l_1}^{l_1,k_1}\left(\left(\frac{k_1}{\lambda_1}\right)^{k_1}\left(\frac{s}{l_1}\right)^{l_1}\left|\begin{array}{c} 1-\Delta(k_1,0) \\ 1-\Delta\left(l_1,1-\frac{\alpha_1\mu_1}{2}\right)\end{array}\right.\right), \quad \frac{l_1}{k_1}=\frac{\alpha_1}{2} \tag{19}$$

$$\Phi_{\bar{Y}}(s) = \frac{\alpha_2 \lambda_2^{\mu_2} k_2^{\frac{1}{2}} l_2^{-\frac{\alpha_2\mu_2+1}{2}} s^{\frac{\alpha_2\mu_2}{2}}}{2\Gamma(\mu_2)(2\pi)^{\frac{l_2+k_2-2}{2}}} G_{0,k_2+l_2}^{k_2+l_2,0}\left(\left(\frac{\lambda_2}{k_2}\right)^{k_2}\left(\frac{s}{l_2}\right)^{l_2}\left|\begin{array}{c} - \\ \Delta(k_2,0),\Delta\left(l_2,-\frac{\alpha_2\mu_2}{2}\right)\end{array}\right.\right), \quad \frac{l_2}{k_2}=\frac{\alpha_2}{2} \tag{20}$$

$$\Phi_{\mathcal{A}}(s) = \frac{\alpha_1 \lambda_1^{\mu_1}}{2\Gamma(\mu_1)(2\pi)^{\frac{l_1+k_1-2}{2}}} \sqrt{\frac{k_1}{l_1}}\left(\frac{2\theta\eta P_S}{l_1}s\right)^{-\frac{\alpha_1\mu_1}{2}} G_{k_1,l_1}^{l_1,k_1}\left(\left(\frac{k_1}{\lambda_1}\right)^{k_1}\left(\frac{2\theta\eta P_S}{l_1}\right)^{l_1} s^{l_1}\left|\begin{array}{c} 1-\Delta(k_1,0) \\ 1-\Delta\left(l_1,1-\frac{\alpha_1\mu_1}{2}\right)\end{array}\right.\right) \tag{21}$$

$$\Phi_{\mathcal{B}+a_3}(s) = \frac{\alpha_2 \lambda_2^{\mu_2}}{2\Gamma(\mu_2)(2\pi)^{\frac{l_2+k_2-2}{2}}} \sqrt{\frac{k_2}{l_2}}\left(\frac{(1-\eta)d_1^{m_1}d_2^{m_2}\sigma_D^2}{l_2}\right)^{\frac{\alpha_2\mu_2}{2}} s^{\frac{\alpha_2\mu_2}{2}} \exp\left(-2\theta\eta d_1^{m_1}\sigma_R^2 s\right)$$
$$\times G_{0,k_2+l_2}^{k_2+l_2,0}\left(\left(\frac{\lambda_2}{k_2}\right)^{k_2}\left(\frac{(1-\eta)d_1^{m_1}d_2^{m_2}\sigma_D^2}{l_2}\right)^{l_2} s^{l_2}\left|\begin{array}{c} - \\ \Delta(k_2,0),\Delta\left(l_2,-\frac{\alpha_2\mu_2}{2}\right)\end{array}\right.\right) \tag{22}$$

$$\mathbb{E}[C_D] = \frac{(1-\eta)\alpha_2 \lambda_2^{\mu_2}}{4\ln(2)\Gamma(\mu_2)(2\pi)^{\frac{k_2+l_2-2}{2}}} \sqrt{\frac{k_2}{l_2}}\left(\frac{d_2^{m_2}\sigma_D^2}{\kappa\sigma_R^2 l_2}\right)^{\frac{\alpha_2\mu_2}{2}} \left[H_{1,k_2+l_2}^{k_2+l_2,1}\left(\left(\frac{\lambda_2}{k_2}\right)^{k_2}\left(\frac{d_2^{m_2}\sigma_D^2}{\kappa\sigma_R^2 l_2}\right)^{l_2}\left|\begin{array}{c}\left(1-\frac{\alpha_2\mu_2}{2},l_2\right)\\(C_1,1),\ldots,(C_{k_2+l_2},1)\end{array}\right.\right)\right.$$
$$-\frac{\alpha_1 \lambda_1^{\mu_1}}{2\Gamma(\mu_1)(2\pi)^{\frac{l_1+k_1-2}{2}}} \sqrt{\frac{k_1}{l_1}}\left(\frac{P_S}{d_1^{m_1}\sigma_R^2 l_1}\right)^{-\frac{\alpha_1\mu_1}{2}} H_{1,0:k_1,l_1:0,l_2+k_2}^{0,1:l_1,k_1:l_2+k_2,0}\left(\begin{array}{c}\left(1+\frac{\alpha_1\mu_1}{2}-\frac{\alpha_2\mu_2}{2}:l_1,l_2\right)\\ -\end{array}\right|$$
$$\left.\begin{array}{c}(A_1,1),\ldots,(A_{k_1},1)\\(B_1,1),\ldots,(B_{l_1},1)\end{array}\left|\begin{array}{c}-\\(C_1,1),\ldots,(C_{k_2+l_2},1)\end{array}\right|\left(\frac{k_1}{\lambda_1}\right)^{k_1}\left(\frac{P_S}{d_1^{m_1}\sigma_R^2 l_1}\right)^{l_1},\left(\frac{\lambda_2}{k_2}\right)^{k_2}\left(\frac{d_2^{m_2}\sigma_D^2}{\kappa\sigma_R^2 l_2}\right)^{l_2}\right)\right] \tag{23}$$

where $\mathcal{R}$ is the minimum required rate while $\gamma_{th}=2^{\frac{2\mathcal{R}}{1-\eta}}-1$ is the corresponding SNR threshold to support $\mathcal{R}$. The fact that Y is a positive value means

$$P_{\text{out}} = \begin{cases} \Pr\left(Y < \frac{\beta_3\gamma_{th}}{\beta_1 X - \beta_2\gamma_{th}}\right), & X > \frac{\beta_2\gamma_{th}}{\beta_1}; \\ \Pr\left(Y > \frac{\beta_3\gamma_{th}}{\beta_1 X - \beta_2\gamma_{th}}\right) = 1, & X < \frac{\beta_2\gamma_{th}}{\beta_1}. \end{cases} \tag{27}$$

Therefore, the OP can be calculated as

$$P_{\text{out}} = \int_0^{\frac{\beta_2\gamma_{th}}{\beta_1}} f_X(r)\mathrm{d}r + \int_{\frac{\beta_2\gamma_{th}}{\beta_1}}^{\infty} f_X(r)F_Y(r)\mathrm{d}r, \tag{28}$$

where the PDF f_X is given by (15) and F_Y is the cumulative distribution function (CDF) of Y which can be expressed as

$$F_Y(r) = \frac{\gamma_{inc}\left(\mu_2,\lambda_2 r^{\frac{\alpha_2}{2}}\right)}{\Gamma(\mu_2)}, \tag{29}$$

where $\gamma_{inc}(s,x) = \int_0^x t^{s-1}\exp(-t)\mathrm{d}t$ indicates the lower incomplete Gamma function [26]. Substituting (15) and (29) into (28), the ergodic OP can be written as

$$P_{\text{out}} = 1 - \frac{\Phi}{\Gamma(\mu_2)}\int_{\frac{\beta_2\gamma_{th}}{\beta_1}}^{\infty} r^{\frac{\alpha_1\mu_1}{2}-1}$$
$$\times \exp\left(-\lambda_1 r^{\frac{\alpha_1}{2}}\right)\gamma_{inc}\left(\mu_2,\lambda_2 r^{\frac{\alpha_2}{2}}\right)\mathrm{d}r, \tag{30}$$

where $\Phi = \frac{\alpha_1\lambda_1^{\mu_1}}{2\Gamma(\mu_1)}$. Then, using $\int_a^{\infty} f_X(r)\mathrm{d}r = 1 - \int_0^a f_X(r)\mathrm{d}r = 1 - F_X(a)$ and the series representation of the lower incomplete Gamma function [26, Eq. (8.339.1) and

Eq. (8.352.6)] where μ_2 is an integer, the OP can be given as

$$P_{\text{out}} = 1 - \Phi\sum_{n=0}^{\mu_2-1}\frac{\lambda_2^n}{n!}\left[1 - \frac{\gamma_{inc}\left(\mu_1,\frac{\beta_2\gamma_{th}}{\beta_1}\right)}{\Gamma(\mu_1)}\right.$$
$$\left.- \int_{\frac{\beta_2\gamma_{th}}{\beta_1}}^{\infty} r^{\frac{\alpha_1\mu_1}{2}+\frac{\alpha_2 n}{2}-1}\exp\left(-\lambda_1 r^{\frac{\alpha_1}{2}}-\lambda_2 r^{\frac{\alpha_2}{2}}\right)\mathrm{d}r\right]. \tag{31}$$

To the best of the authors' knowledge, the OP expression given by (31) does not have a closed-form solution without imposing certain assumptions and, therefore, can only be solved numerically. However, if we assume equal α parameters, this integral can be solved in closed-form as given by (34). It is worthwhile mentioning that, since we do not assume equal μ fading parameters, this assumption allows one to study the mixed channels, i.e., Weibull/Weibull, Rayleigh/Nakagami$-m$ and Nakagami$-m$/Rayleigh with various m values. Therefore, to get a closed-form solution, we assume that $\alpha_1=\alpha_2$. Thus, the integral in (31) can be rewritten as

$$A = \int_{\frac{\beta_2\gamma_{th}}{\beta_1}}^{\infty} r^{\frac{\alpha_1}{2}(\mu_1+n)-1}\exp\left(-r^{\frac{\alpha_1}{2}}(\lambda_1+\lambda_2)\right)\mathrm{d}r. \tag{32}$$

By substituting $t = r^{\frac{\alpha_1}{2}}(\lambda_1+\lambda_2)$ and after some algebraic manipulations, this integral can be written in closed-form as

$$A = \frac{2}{\alpha_1(\lambda_1+\lambda_2)^{\mu_1+n}}\Gamma\left(\mu_1+n,\left(\frac{\beta_2\gamma_{th}}{\beta_1(\lambda_1+\lambda_2)}\right)^{2/\alpha_1}\right), \tag{33}$$

where $\Gamma(s,x) = \int_x^\infty t^{s-1}\exp(-t)\mathrm{d}t$ denotes the upper incomplete Gamma function [26].

Now, after substituting (33) into (31) and some algebraic manipulation, we obtain a closed-form expression of the ergodic OP as in (34), as shown at the top of the next page.

IV. PERFORMANCE ANALYSIS OF THE PSR-BASED SYSTEM

In this protocol, the time frame T is formed by two equal TSs. During the first TS, R assigns a portion of the received signal power for EH (i.e., ρP_S), and the remaining received power, i.e., $(1-\rho)P_S$, is assigned for the $S\text{-to-}R$ data transmission, where ρ is the PS factor as depicted in Fig. 2(b). Therefore, the energy harvester obtains the received signal expressed as

$$\sqrt{\rho}y_R(t) = \sqrt{\frac{\rho P_S}{d_1^{m_1}}}h_1 s(t) + \sqrt{\rho}n_a(t). \quad (35)$$

The amount of the scavenged energy, to be used to amplify and then forward information to D, can be calculated as

$$E_H^{PSR} = \frac{\theta\rho T}{2}\left(\frac{P_S}{d_1^{m_1}}h_1^2 + \sigma_a^2\right). \quad (36)$$

Accordingly, the transmit signal at R is given as

$$s_R(t) = \sqrt{\frac{(1-\rho)P_S P_R}{d_1^{m_1}}}Gh_1 s(t) + \sqrt{P_R}Gn_R(t), \quad (37)$$

where $G = 1/\sqrt{\frac{(1-\rho)P_S}{d_1^{m_1}}h_1^2 + \sigma_R^2}$ denotes the relay gain and $n_R(t) = \sqrt{1-\rho}n_a(t)+n_c(t)$. With this in mind, the received signal at D can be expressed as

$$y_D(t) = \sqrt{\frac{P_R}{d_2^{m_2}}}Gh_2\left(\sqrt{\frac{(1-\rho)P_S}{d_1^{m_1}}}h_1 s(t) + n_R(t)\right) + n_D(t). \quad (38)$$

Due to $P_R = \frac{2E_H^{PSR}}{T}$, the relay transmit power can be given using (36) as

$$P_R = \theta\rho\left(\frac{P_S}{d_1^{m_1}}h_1^2 + \sigma_a^2\right). \quad (39)$$

Substituting (39) into (38), we express the SNR at D as

$$\gamma_D = \frac{\theta\rho(1-\rho)P_S h_1^2 h_2^2}{d_1^{m_1}\left(\theta\rho\sigma_c^2 h_2^2 + \theta\rho(1-\rho)\sigma_a^2 h_2^2 + (1-\rho)d_2^{m_2}\sigma_D^2\right)}. \quad (40)$$

A. Ergodic Capacity

Using $b_1 = \theta\rho(1-\rho)P_S$, $b_2 = (1-\rho)d_1^{m_1}d_2^{m_2}\sigma_D^2$, $b_3 = \theta\rho d_1^{m_1}\sigma_c^2$, $b_4 = \theta\rho(1-\rho)d_1^{m_1}\sigma_a^2$, $\mathcal{K} = b_1 X$ and $\mathcal{L} = b_2\bar{Y}$, the SNR in (40) can be rewritten as

$$\gamma_D = \frac{\mathcal{K}}{\mathcal{L} + b_3 + b_4}. \quad (41)$$

Substituting (41) into (3), we express the EC as

$$\mathbb{E}[C_D] = \frac{1}{2}\mathbb{E}\left[\log_2\left(1 + \frac{\mathcal{K}}{\mathcal{L} + b_3 + b_4}\right)\right], \quad (42)$$

which, using (13), can also be written as

$$\mathbb{E}[C_D] = \frac{1}{2\ln(2)}\int_0^\infty \frac{1}{s}\left(1 - \Phi_{\mathcal{K}}(s)\right)\Phi_{\mathcal{L}+b_3+b_4}(s)\mathrm{d}s, \quad (43)$$

where $\Phi_{\mathcal{K}}(s) = \Phi_X(b_1 s)$ and $\Phi_{\mathcal{L}+b_3+b_4}(s) = \Phi_{\bar{Y}}(b_2 s)\exp(-b_3 s)\exp(-b_4 s)$ denote the corresponding MGFs, shown at the top of the next page.

Finally, the end-to-end EC of the PSR-based system can be given as in (46), where $\zeta = \frac{\theta\rho}{(1-\rho)}$ and $\bar{\sigma}_R^2 = \sigma_c^2 + (1-\rho)\sigma_a^2$.

B. Ergodic Outage Probability

The SNR at D given in (40) can be given as

$$\gamma_D = \frac{\delta_1 XY}{\delta_2 Y + \delta_3}, \quad (47)$$

where $\delta_1 = \rho(1-\rho)\theta P_S$, $\delta_2 = \theta d_1^m\rho\left(\sigma_c^2 + (1-\rho)\sigma_a^2\right)$, $\delta_3 = (1-\rho)d_1^m d_2^m\sigma_D^2$, $X = h_1^2$ and $Y = h_2^2$.

The ergodic OP can be expressed, using (2) and (40), as

$$P_{\text{out}}^{\text{PSR}} = \Pr\left(\frac{\delta_1 XY}{\delta_2 Y + \delta_3} < \gamma_{th}\right) = \Pr\left(Y < \frac{\delta_3\gamma_{th}}{\delta_1 X - \delta_2\gamma_{th}}\right), \quad (48)$$

where $\gamma_{th} = 2^{2\mathcal{R}} - 1$ is the corresponding SNR threshold to support $\mathcal{R}$. The fact that Y is a positive value means

$$P_{\text{out}}^{\text{PSR}} = \begin{cases} \Pr\left(Y < \frac{\delta_3\gamma_{th}}{\delta_1 X - \delta_2\gamma_{th}}\right), & X > \frac{\delta_2\gamma_{th}}{\delta_1}; \\ \Pr\left(Y > \frac{\delta_3\gamma_{th}}{\delta_1 X - \delta_2\gamma_{th}}\right) = 1, & X < \frac{\delta_2\gamma_{th}}{\delta_1}. \end{cases} \quad (49)$$

Therefore, the OP can be calculated as

$$P_{\text{out}}^{\text{PSR}} = \int_0^{\frac{\delta_2\gamma_{th}}{\delta_1}} f_X(r)\mathrm{d}r + \int_{\frac{\delta_2\gamma_{th}}{\delta_1}}^\infty f_X(r)F_Y(r)\mathrm{d}r. \quad (50)$$

Substituting (15) and (29) into (50), the OP can be given as

$$P_{\text{out}}^{\text{PSR}} = 1 - \frac{\Phi}{\Gamma(\mu_2)}\int_{\frac{\delta_2\gamma_{th}}{\delta_1}}^\infty r^{\frac{\alpha_1\mu_1}{2}-1}$$
$$\times \exp\left(-\lambda_1 r^{\frac{\alpha_1}{2}}\right)\gamma_{inc}\left(\mu_2, \lambda_2 r^{\frac{\alpha_2}{2}}\right)\mathrm{d}r. \quad (51)$$

Then, the OP can be rewritten as

$$P_{\text{out}}^{\text{PSR}} = 1 - \Phi\sum_{n=0}^{\mu_2-1}\frac{\lambda_2^n}{n!}\left[1 - \frac{\gamma_{inc}\left(\mu_1, \frac{\delta_2\gamma_{th}}{\delta_1}\right)}{\Gamma(\mu_1)}\right.$$
$$\left. - \int_{\frac{\delta_2\gamma_{th}}{\delta_1}}^\infty r^{\frac{\alpha_1\mu_1}{2}+\frac{\alpha_2 n}{2}-1}\exp\left(-\lambda_1 r^{\frac{\alpha_1}{2}} - \lambda_2 r^{\frac{\alpha_2}{2}}\right)\mathrm{d}r\right]. \quad (52)$$

To get a closed-form solution, the integral in (52) can be rewritten as

$$B = \int_{\frac{\delta_2\gamma_{th}}{\delta_1}}^\infty r^{\frac{\alpha_1}{2}(\mu_1+n)-1}\exp\left(-r^{\frac{\alpha_1}{2}}(\lambda_1 + \lambda_2)\right)\mathrm{d}r. \quad (53)$$

By substituting $t = r^{\frac{\alpha_1}{2}}(\lambda_1 + \lambda_2)$ and after some algebraic manipulation, this integral can be given in closed-form as

$$B = \frac{2}{\alpha_1(\lambda_1 + \lambda_2)^{\mu_1+n}}\Gamma\left(\mu_1 + n, \left(\frac{\delta_2\gamma_{th}}{\delta_1(\lambda_1 + \lambda_2)}\right)^{2/\alpha_1}\right). \quad (54)$$

$$P_{\text{out}}^{\text{TSR}} = 1 - \frac{\alpha_1\lambda_1^{\mu_1}}{2\Gamma(\mu_1)}\sum_{n=0}^{\mu_2-1}\frac{\lambda_2^n}{n!}\left[1 - \frac{\gamma_{inc}\left(\mu_1, \frac{d_1^{m_1}\sigma_R^2\gamma_{th}}{P_S}\right)}{\Gamma(\mu_1)} - \frac{2}{\alpha_1\left(\lambda_1+\lambda_2\right)^{\mu_1+n}}\Gamma\left(\mu_1+n, \left(\frac{d_1^{m_1}\sigma_R^2\gamma_{th}}{P_S\left(\lambda_1+\lambda_2\right)}\right)^{2/\alpha_1}\right)\right] \quad (34)$$

$$\Phi_{\mathcal{K}}(s) = \sqrt{\frac{k_1}{l_1}}\left(\frac{\theta\rho(1-\rho)P_S}{l_1}\right)^{-\frac{\alpha_1\mu_1}{2}}s^{-\frac{\alpha_1\mu_1}{2}}\frac{\alpha_1\lambda_1^{\mu_1}G_{k_1,l_1}^{l_1,k_1}\left(\left(\frac{k_1}{\lambda_1}\right)^{k_1}\left(\frac{\theta\rho(1-\rho)P_S}{l_1}\right)^{l_1}s^{l_1}\left|\begin{array}{c}1-\Delta\left(k_1,0\right)\\1-\Delta\left(l_1,1-\frac{\alpha_1\mu_1}{2}\right)\end{array}\right.\right)}{2\Gamma(\mu_1)\left(2\pi\right)^{\frac{l_1+k_1-2}{2}}} \quad (44)$$

$$\Phi_{\mathcal{L}+b_3+b_4}(s) = \frac{\alpha_2\lambda_2^{\mu_2}}{2\Gamma(\mu_2)\left(2\pi\right)^{\frac{l_2+k_2-2}{2}}}\sqrt{\frac{k_2}{l_2}}\left(\frac{(1-\rho)d_1^{m_1}d_2^{m_2}\sigma_D^2}{l_2}\right)^{\frac{\alpha_2\mu_2}{2}}s^{\frac{\alpha_2\mu_2}{2}}\exp\left(-\theta\rho d_1^{m_1}\sigma_c^2 s\right)\exp\left(-\theta\rho(1-\rho)d_1^{m_1}\sigma_a^2 s\right)$$
$$\times G_{0,k_2+l_2}^{k_2+l_2,0}\left(\left(\frac{\lambda_2}{k_2}\right)^{k_2}\left(\frac{(1-\rho)d_1^{m_1}d_2^{m_2}\sigma_D^2}{l_2}\right)^{l_2}s^{l_2}\left|\begin{array}{c}-\\\Delta\left(k_2,0\right),\Delta\left(l_2,-\frac{\alpha_2\mu_2}{2}\right)\end{array}\right.\right) \quad (45)$$

$$\mathbb{E}[C_D] = \frac{\alpha_2\lambda_2^{\mu_2}}{4\ln(2)\Gamma(\mu_2)(2\pi)^{\frac{l_2+k_2-2}{2}}}\sqrt{\frac{k_2}{l_2}}\left(\frac{d_2^{m_2}\sigma_D^2}{\zeta\bar\sigma_R^2 l_2}\right)^{\frac{\alpha_2\mu_2}{2}}\left[H_{1,k_2+l_2}^{k_2+l_2,1}\left(\left(\frac{\lambda_2}{k_2}\right)^{k_2}\left(\frac{d_2^{m_2}\sigma_D^2}{\zeta\bar\sigma_R^2 l_2}\right)^{l_2}\left|\begin{array}{c}(1-\frac{\alpha_2\mu_2}{2},l_2)\\(C_1,1),\ldots,(C_{k_2+l_2},1)\end{array}\right.\right)$$
$$-\frac{\alpha_1\lambda_1^{\mu_1}}{2\Gamma(\mu_1)(2\pi)^{\frac{l_1+k_1-2}{2}}}\sqrt{\frac{k_1}{l_1}}\left(\frac{(1-\rho)P_S}{d_1^{m_1}\bar\sigma_R^2 l_1}\right)^{-\frac{\alpha_1\mu_1}{2}}H_{1,0:k_1,l_1:0,k_2+l_2}^{0,1:l_1,k_1:k_2+l_2,0}\left(\begin{array}{c}(1+\frac{\alpha_1\mu_1}{2}-\frac{\alpha_2\mu_2}{2}:l_1,l_2)\\-\end{array}\right|$$
$$\left.\begin{array}{c}(A_1,1),\ldots,(A_{k_1},1)\\(B_1,1),\ldots,(B_{l_1},1)\end{array}\right|\left.\begin{array}{c}-\\(C_1,1),\ldots,(C_{k_2+l_2},1)\end{array}\right|\left(\frac{k_1}{\lambda_1}\right)^{k_1}\left(\frac{(1-\rho)P_S}{d_1^{m_1}\bar\sigma_R^2 l_1}\right)^{l_1},\left(\frac{\lambda_2}{k_2}\right)^{k_2}\left(\frac{d_2^{m_2}\sigma_D^2}{\zeta\bar\sigma_R^2 l_2}\right)^{l_2}\right)\right] \quad (46)$$

Now, after substituting (54) into (52), we obtain a closed-form expression of the ergodic OP as in (55).

V. PERFORMANCE ANALYSIS OF THE IRR-BASED SYSTEM

Similar to the PSR protocol, the IRR one equally divides the time frame T into two consecutive TSs. However, the first TS is simultaneously allocated for EH and information transmission; see Fig. 2(c). Similar to the procedure in Section IV, the SNR at D can be obtained as

$$\gamma_D = \frac{\theta P_S h_1^2 h_2^2}{\theta d_1^{m_1}\sigma_R^2 h_2^2 + d_1^{m_1}d_2^{m_2}\sigma_D^2}. \quad (56)$$

Letting $c_1 = \theta P_s$, $c_2 = d_1^{m_1}d_2^{m_2}\sigma_D^2$, $c_3 = \theta d_1^{m_1}\sigma_R^2$, $\mathcal{E} = c_1 X$ and $\mathcal{F} = c_2\bar{Y}$, (56) can be rewritten as

$$\gamma_D = \frac{\mathcal{E}}{\mathcal{F}+c_3}. \quad (57)$$

A. Ergodic Capacity

Using (57), the EC can be evaluated as

$$\mathbb{E}[C_D] = \frac{1}{2}\mathbb{E}\left[\log_2\left(1+\frac{\mathcal{E}}{\mathcal{F}+c_3}\right)\right]$$
$$= \frac{1}{2\ln(2)}\int_0^\infty\frac{1}{s}\left(1-\Phi_{\mathcal{E}}(s)\right)\Phi_{\mathcal{F}+c_3}(s)ds, \quad (58)$$

where $\Phi_{\mathcal{E}}(s) = \Phi_X(c_1 s)$ and $\Phi_{\mathcal{F}+c_3}(s) = \Phi_{\bar{Y}}(c_2 s)\exp(-c_3 s)$ denote the corresponding MGFs, shown at the top of the next page.

Finally, following the same approach, the end-to-end EC of the IRR-based system can be expressed as in (61), shown at the top of the next page.

B. Ergodic Outage Probability

The SNR at D in (56) can be re-expressed as

$$\gamma_D = \frac{\epsilon_1 XY}{\epsilon_2 Y + \epsilon_3}, \quad (62)$$

where $\epsilon_1 = \theta P_S$, $\epsilon_2 = \theta d_1^{m_1}\sigma_R^2$, $\epsilon_3 = d_1^{m_1}d_2^{m_2}\sigma_D^2$.

The ergodic OP can be expressed, using (2) and (62), as

$$P_{\text{out}}^{\text{IRR}} = \Pr\left(\frac{\epsilon_1 XY}{\epsilon_2 Y+\epsilon_3}<\gamma_{th}\right) = \Pr\left(Y<\frac{\epsilon_3\gamma_{th}}{\epsilon_1 X-\epsilon_2\gamma_{th}}\right). \quad (63)$$

The fact that Y is a positive value means

$$P_{\text{out}}^{\text{IRR}} = \begin{cases}\Pr\left(Y<\frac{\epsilon_3\gamma_{th}}{\epsilon_1 X-\epsilon_2\gamma_{th}}\right), & X>\frac{\epsilon_2\gamma_{th}}{\epsilon_1};\\\Pr\left(Y>\frac{\epsilon_3\gamma_{th}}{\epsilon_1 X-\epsilon_2\gamma_{th}}\right)=1, & X<\frac{\epsilon_2\gamma_{th}}{\epsilon_1}.\end{cases} \quad (64)$$

Therefore, the OP can be calculated as

$$P_{\text{out}}^{\text{IRR}} = \int_0^{\frac{\epsilon_2\gamma_{th}}{\epsilon_1}}f_X(r)\mathrm{d}r + \int_{\frac{\epsilon_2\gamma_{th}}{\epsilon_1}}^\infty f_X(r)F_Y(r)\mathrm{d}r$$
$$= 1 - \frac{\Phi}{\Gamma(\mu_2)}\int_{\frac{\epsilon_2\gamma_{th}}{\epsilon_1}}^\infty r^{\frac{\alpha_1\mu_1}{2}-1}$$
$$\times\exp\left(-\lambda_1 r^{\frac{\alpha_1}{2}}\right)\gamma_{inc}\left(\mu_2,\lambda_2 r^{\frac{\alpha_2}{2}}\right)\mathrm{d}r. \quad (65)$$

Then, the OP can be rewritten as

$$P_{\text{out}}^{\text{IRR}} = 1 - \Phi\sum_{n=0}^{\mu_2-1}\frac{\lambda_2^n}{n!}\left[1-\frac{\gamma_{inc}\left(\mu_1,\frac{\epsilon_2\gamma_{th}}{\epsilon_1}\right)}{\Gamma(\mu_1)}\right.$$

$$P_{\text{out}}^{\text{PSR}} = 1 - \frac{\alpha_1 \lambda_1^{\mu_1}}{2\Gamma(\mu_1)} \sum_{n=0}^{\mu_2-1} \frac{\lambda_2^n}{n!} \left[1 - \frac{\gamma_{inc}\left(\mu_1, \frac{d_1^{m_1}\left(\sigma_c^2+(1-\rho)\sigma_a^2\right)\gamma_{th}}{P_S(1-\rho)}\right)}{\Gamma(\mu_1)} - \frac{2\Gamma\left(\mu_1+n, \left(\frac{d_1^{m_1}\left(\sigma_c^2+(1-\rho)\sigma_a^2\right)\gamma_{th}}{P_S(1-\rho)(\lambda_1+\lambda_2)}\right)^{2/\alpha_1}\right)}{\alpha_1\left(\lambda_1+\lambda_2\right)^{\mu_1+n}} \right] \tag{55}$$

$$\Phi_{\mathcal{E}}(s) = \frac{\alpha_1 \lambda_1^{\mu_1}}{2\Gamma(\mu_1)(2\pi)^{\frac{l_1+k_1-2}{2}}} \sqrt{\frac{k_1}{l_1}} \left(\frac{\theta P_S}{l_1}\right)^{-\frac{\alpha_1\mu_1}{2}} s^{-\frac{\alpha_1\mu_1}{2}} G_{k_1,l_1}^{l_1,k_1}\left(\left(\frac{k_1}{\lambda_1}\right)^{k_1}\left(\frac{\theta P_S}{l_1}\right)^{l_1} s^{l_1} \,\middle|\, \begin{array}{c} 1-\Delta(k_1,0) \\ 1-\Delta\left(l_1, 1-\frac{\alpha_1\mu_1}{2}\right) \end{array}\right) \tag{59}$$

$$\Phi_{\mathcal{F}+c_3}(s) = \frac{\alpha_2 \lambda_2^{\mu_2}}{2\Gamma(\mu_2)(2\pi)^{\frac{l_2+k_2-2}{2}}} \sqrt{\frac{k_2}{l_2}} \left(\frac{d_1^{m_1} d_2^{m_2}\sigma_D^2}{l_2}\right)^{\frac{\alpha_2\mu_2}{2}} s^{\frac{\alpha_2\mu_2}{2}} \exp\left(-\theta d_1^{m_1}\sigma_R^2 s\right)$$
$$\times G_{0,k_2+l_2}^{k_2+l_2,0}\left(\left(\frac{\lambda_2}{k_2}\right)^{k_2}\left(\frac{d_1^{m_1}d_2^{m_2}\sigma_D^2}{l_2}\right)^{l_2} s^{l_2} \,\middle|\, \begin{array}{c} - \\ \Delta(k_2,0), \Delta\left(l_2, -\frac{\alpha_2\mu_2}{2}\right) \end{array}\right) \tag{60}$$

$$\mathbb{E}[C_D] = \frac{\alpha_2 \lambda_2^{\mu_2}}{4\ln(2)\Gamma(\mu_2)(2\pi)^{\frac{l_2+k_2-2}{2}}} \sqrt{\frac{k_2}{l_2}} \left(\frac{d_2^{m_2}\sigma_D^2}{\theta\sigma_R^2 l_2}\right)^{\frac{\alpha_2\mu_2}{2}} \left[H_{1,k_2+l_2}^{k_2+l_2,1}\left(\left(\frac{\lambda_2}{k_2}\right)^{k_2}\left(\frac{d_2^{m_2}\sigma_D^2}{\theta\sigma_R^2 l_2}\right)^{l_2} \,\middle|\, \begin{array}{c} \left(1-\frac{\alpha_2\mu_2}{2}, l_2\right) \\ (C_1,1),\ldots,(C_{k_2+l_2},1) \end{array}\right) \right.$$
$$- \frac{\alpha_1 \lambda_1^{\mu_1}}{2\Gamma(\mu_1)(2\pi)^{\frac{l_1+k_1-2}{2}}} \sqrt{\frac{k_1}{l_1}} \left(\frac{P_S}{d_1^{m_1}\sigma_R^2 l_1}\right)^{-\frac{\alpha_1\mu_1}{2}} H_{1,0:k_1:k_2+l_2,0}^{0,1:l_1,k_1:k_2+l_2,0}\left(\begin{array}{c} \left(1+\frac{\alpha_1\mu_1}{2}-\frac{\alpha_2\mu_2}{2}:l_1,l_2\right) \\ - \end{array} \,\middle|\, \right.$$
$$\left. \begin{array}{c} (A_1,1),\ldots,(A_{k_1},1) \\ (B_1,1),\ldots,(B_{l_1},1) \end{array} \,\middle|\, \begin{array}{c} - \\ (C_1,1),\ldots,(C_{k_2+l_2},1) \end{array} \,\middle|\, \left(\frac{k_1}{\lambda_1}\right)^{k_1}\left(\frac{P_S}{d_1^{m_1}\sigma_R^2 l_1}\right)^{l_1}, \left(\frac{\lambda_2}{k_2}\right)^{k_2}\left(\frac{d_2^{m_2}\sigma_D^2}{\theta\sigma_R^2 l_2}\right)^{l_2}\right) \right] \tag{61}$$

$$\left. - \int_{\frac{\epsilon_2\gamma_{th}}{\epsilon_1}}^{\infty} r^{\frac{\alpha_1\mu_1}{2}+\frac{\alpha_2 n}{2}-1} \exp\left(-\lambda_1 r^{\frac{\alpha_1}{2}} - \lambda_2 r^{\frac{\alpha_2}{2}}\right) \mathrm{d}r \right]. \tag{66}$$

Similar to (53), the integral in (66) can be rewritten as

$$C = \int_{\frac{\epsilon_2\gamma_{th}}{\epsilon_1}}^{\infty} r^{\frac{\alpha_1}{2}(\mu_1+n)-1} \exp\left(-r^{\frac{\alpha_1}{2}}(\lambda_1+\lambda_2)\right) \mathrm{d}r. \tag{67}$$

By substituting $t = r^{\frac{\alpha_1}{2}}(\lambda_1+\lambda_2)$, this integral can be given in closed-form as

$$C = \frac{2}{\alpha_1(\lambda_1+\lambda_2)^{\mu_1+n}} \Gamma\left(\mu_1+n, \left(\frac{\epsilon_2\gamma_{th}}{\epsilon_1(\lambda_1+\lambda_2)}\right)^{2/\alpha_1}\right). \tag{68}$$

Now, after substituting (68) into (66), we obtain a closed-form expression for the ergodic OP as in (69), as shown at the top of the next page. For more details see Appendix A.

VI. NUMERICAL AND SIMULATION RESULTS

In this section, we present numerical examples for the derived expressions. The adopted system parameters in our evaluations in this section are as follows: $G = 1$, $m_1 = m_2 = 2.7$, $\sigma_R = \sigma_D = 0.02$ W and $\sigma_a = \sigma_c = \sigma_R/2$. By setting various α and μ parameters, we get the Nakagami-m ($\alpha = 2$), Rayleigh ($\alpha = 2$ and $\mu = 1$) and Weibull ($\mu = 1$) channels.

A. Ergodic Capacity

In this section, the impact of η and ρ on the EC for the PSR and TSR protocols is investigated. Specifically, the

following system parameters are considered: $\theta = \{0.5; 1\}$, $d_1 = d_2 = 3$ m and $P_S = 1$ W. Fig. 3 presents some analytical and simulation results for the ECs built versus ρ and η for the considered fading models. The analytical results for the TSR and PSR protocols are plotted using Eqs. (23) and (46), respectively. Considering the TSR protocol, when η is small, no sufficient time is dedicated for harvesting purposes, and, thus, the relay is able to harvest only a small power portion, which, in turn, leads to poor capacity. On the other hand, being η too large results in the excessive amount of the scavenged power at the cost of time devoted for communication which apparently leads to poor capacity. The PSR case also applies the similar justification. It is worth noting that η and ρ are the main parameters defining the performance of these protocols and therefore optimizing them will maximize the system performance.

B. System Optimization

Next, we find optimal η^* and ρ^* values for $\theta = 1$ and $P_S = \{1; 5\}$ W to analyze the performance of the optimized TSR and PSR protocols by solving $d\{\mathbb{E}[C_D]\}/d\eta = 0$ and $d\{\mathbb{E}[C_D]\}/d\rho = 0$. It is worth mentioning that these equations can be easily calculated numerically using software tools such as $Mathematica$ since it is difficult to obtain their closed-form solutions.

Fig. 4 illustrates the maximum achievable EC for η^* and ρ^* as a function of d_2 (the R-to-D distance) when the end-to-end S-to-D distance equals 10 m. One can observe that

$$P_{\text{out}}^{\text{IRR}} = 1 - \frac{\alpha_1 \lambda_1^{\mu_1}}{2\Gamma(\mu_1)} \sum_{n=0}^{\mu_2-1} \frac{\lambda_2^n}{n!} \left[1 - \frac{\gamma_{inc}\left(\mu_1, \frac{d_1^{m_1}\sigma_R^2\gamma_{th}}{P_S}\right)}{\Gamma(\mu_1)} - \frac{2}{\alpha_1(\lambda_1+\lambda_2)^{\mu_1+n}}\Gamma\left(\mu_1+n, \left(\frac{d_1^{m_1}\sigma_R^2\gamma_{th}}{P_S(\lambda_1+\lambda_2)}\right)^{2/\alpha_1}\right) \right] \quad (69)$$

(a) Rayleigh ($\alpha = 2$ and $\mu = 1$).

(b) Nakagami-m ($\alpha = 2$ and $\mu = m = 2$).
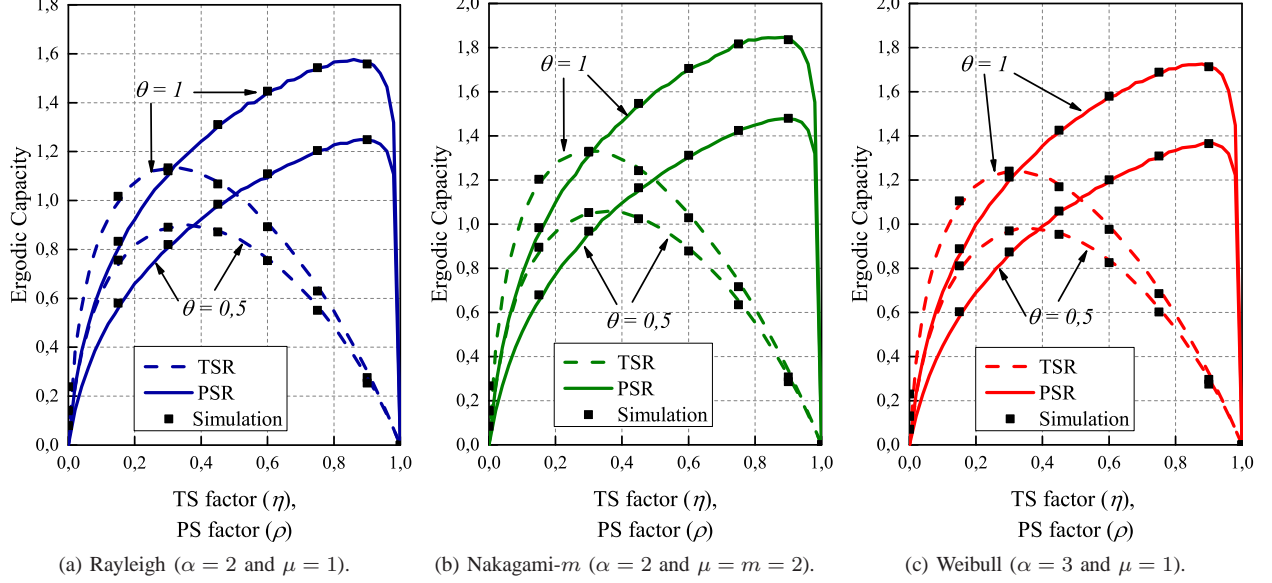
(c) Weibull ($\alpha = 3$ and $\mu = 1$).

Fig. 3. Ergodic capacity versus the EH TS and PS factors for the TSR- and PSR-based systems with different α and μ values.

(a) Rayleigh ($\alpha = 2$ and $\mu = 1$).

(b) Nakagami-m ($\alpha = 2$ and $\mu = m = 2$).
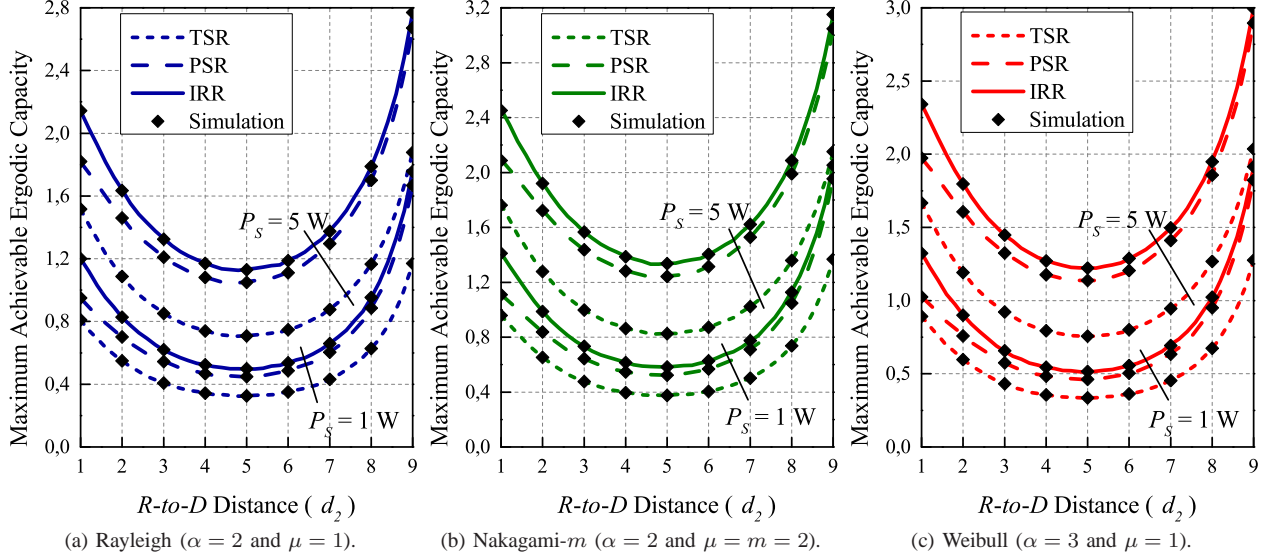
(c) Weibull ($\alpha = 3$ and $\mu = 1$).

Fig. 4. Ergodic capacity versus d_2 ($d_2 = 10 - d_1$) for the IRR- and optimized TSR/PSR-based systems with different α and μ fading parameters when $P_S = \{1; 5\}$ W.

the optimized PSR protocol always has better performance than the optimized TSR one irrespective of the location of R, while the best performance is provided by the IRR-based system. At $d_2 = 9$ m, the performance of the optimized PSR protocol almost achieves the EC of the IRR one. Moreover, the worse performance for the three systems is detected when R resides midway between S and D. This can be explained

by the fact that EH, in this case, attains its peak values which dramatically affect the time devoted for communication and hence the overall EC.

C. Ergodic Outage Probability

We consider in our investigations in this section the following parameters: $P_S = 1$ W, $\theta = 0.7$, $\sigma_R = \sigma_D = 0.02$ W,
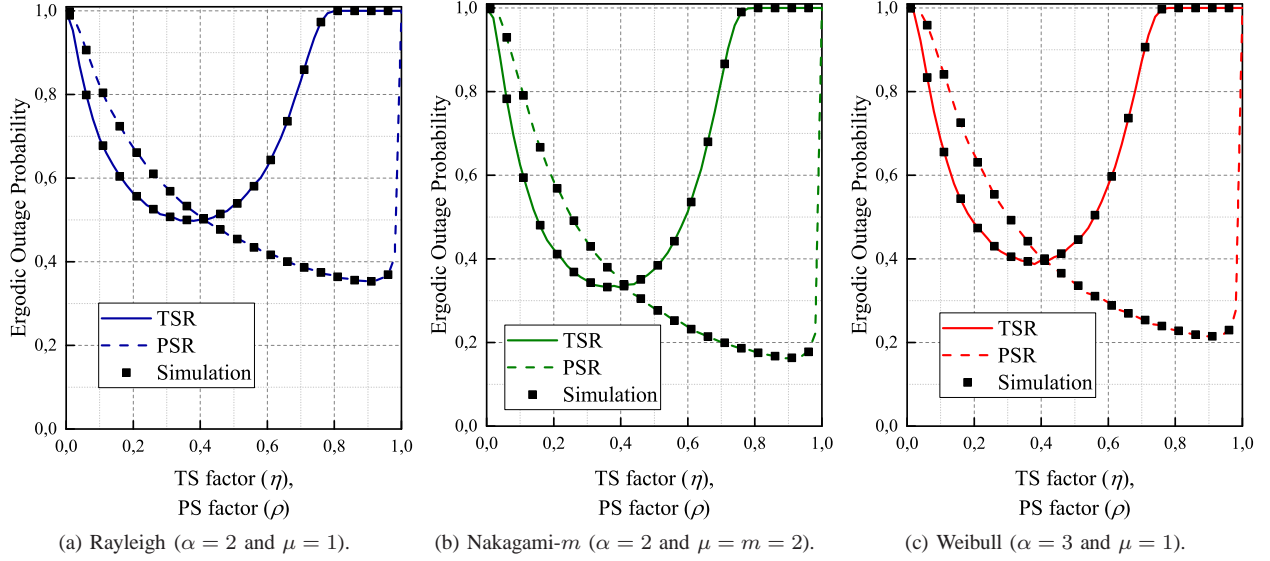
(a) Rayleigh ($\alpha = 2$ and $\mu = 1$).   (b) Nakagami-m ($\alpha = 2$ and $\mu = m = 2$).   (c) Weibull ($\alpha = 3$ and $\mu = 1$).

Fig. 5. Ergodic OP versus the EH TS and PS factors for the TSR- and PSR-based systems with different α and μ values.

(a) Rayleigh ($\alpha = 2$ and $\mu = 1$).   (b) Nakagami-m ($\alpha = 2$ and $\mu = m = 2$).   (c) Weibull ($\alpha = 3$ and $\mu = 1$).
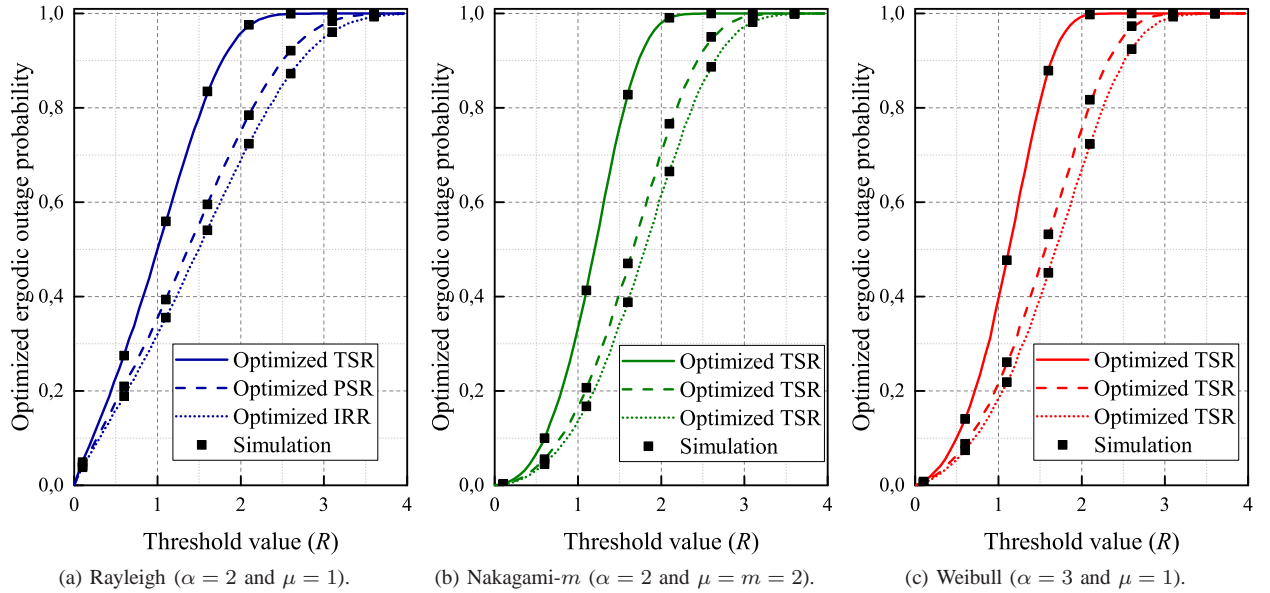
Fig. 6. Optimized ergodic OP versus $\mathcal{R}$ for the three EH protocols over different α-μ fading channels: (a) Rayleigh, (b) Nakagami-m and (c) Weibull.

$\sigma_a = \sigma_c = \sigma_R/2$ W, $\alpha_1 = \alpha_2$, $\mu_1 = \mu_2$ and $d_1 = d_2 = 3$ m.

Fig. 5 illustrates some simulation and analytical results for the ergodic OP given by Eqs. (71)-(73) for the PSR and TSR-based systems with respect to η and ρ. It can be noticed that the performance improves when η and ρ increase. However, when η and ρ approach either 0 or 1, the OP significantly deteriorates. This is because the amount of harvested power is either excessively too large or too small which negatively affects the information transmission time. This implies that the EH time and PS factors must be optimized for best performance.

Fig. 6 presents results for the optimal ergodic OP versus $\mathcal{R}$ for the PSR and TSR protocols. Initially, we find optimal ρ^* and η^* by solving the following $\mathrm{d}P_{\mathrm{out}}(\eta)/\mathrm{d}\eta = 0$ and $\mathrm{d}P_{\mathrm{out}}(\rho)/\mathrm{d}\rho = 0$. Again, only numerical solution are possible for these equations which are obtained using software tools. Clearly, the IRR protocol provides the best OP and the optimized PSR relaying system outperforms the TSR one for the considered configuration.

Now, to illustrate the impact of the fading parameters on the system performance, we plot in Fig. 7 the ergodic OP for the IRR protocol versus α and μ fading parameters. It is evident that the ergodic OP improves as we increase the values of α and/or μ. This is because of the fact that the parameters α and ρ are directly related to the power exponent and the number of multi-path components of the channel, respectively [33].
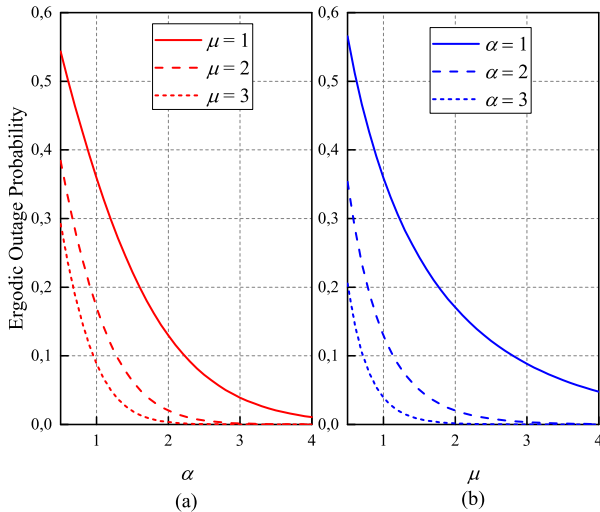
Fig. 7. Ergodic OP versus α and μ for the IRR protocol.

The ergodic OP for the Rayleigh ($\alpha = 2$ and $\mu = 1$), Nakagami-m ($\alpha = 2$ and $\mu = 2$) and Weibull ($\alpha = 3$ and $\mu = 1$) fading channels can be respectively written as

$$P_{\text{out}}^{\text{R}} = 1 - \lambda_1^{\text{R}} \left[1 - \gamma_{inc} \left(1, \frac{\beta_2 \gamma_{th}}{\beta_1} \right) \right.$$
$$\left. - \frac{\Gamma \left(1, \frac{\beta_2 \gamma_{th}}{\beta_1 \left(\sum_{i=\{1,2\}} \lambda_i^{\text{R}} \right)} \right)}{\sum_{i=\{1,2\}} \lambda_i^{\text{R}}} \right], \quad \lambda_i^{\text{R}} = \frac{1}{\hat{r}^2}, \quad (71)$$

$$P_{\text{out}}^{\text{N}} = 1 - \left(\lambda_1^{\text{N}} \right)^2 \sum_{n=0}^{1} \frac{\left(\lambda_2^{\text{N}} \right)^n}{n!} \left[1 - \gamma_{inc} \left(2, \frac{\beta_2 \gamma_{th}}{\beta_1} \right) \right.$$
$$\left. - \frac{\Gamma \left(2 + n, \frac{\beta_2 \gamma_{th}}{\beta_1 \left(\sum_{i=\{1,2\}} \lambda_i^{\text{N}} \right)} \right)}{\left(\sum_{i=\{1,2\}} \lambda_i^{\text{N}} \right)^{2+n}} \right], \quad \lambda_i^{\text{N}} = \frac{2}{\hat{r}^2}, \quad (72)$$

$$P_{\text{out}}^{\text{W}} = 1 - \frac{3 \lambda_1^{\text{W}}}{2} \left[1 - \gamma_{inc} \left(1, \frac{\beta_2 \gamma_{th}}{\beta_1} \right) \right.$$
$$\left. - \frac{2 \Gamma \left(1, \left(\frac{\beta_2 \gamma_{th}}{\beta_1 \left(\sum_{i=\{1,2\}} \lambda_i^{\text{W}} \right)} \right)^{2/3} \right)}{3 \left(\sum_{i=\{1,2\}} \lambda_i^{\text{W}} \right)} \right], \quad \lambda_i^{\text{W}} = \frac{1}{\hat{r}^3}. \quad (73)$$

VII. Conclusion

In this paper, we investigated the EC and OP performance metrics of different wireless powered AF relaying protocols over i.n.i.d. α-μ channels, i.e., Weibull, Nakagami-m and Rayleigh channels. We obtained unified exact closed-form analytical expressions in terms of the H-functions for the EC and OP performance metrics verified by Monte Carlo simulations for the considered EH protocols, i.e., IRR, PSR and TRR. The results revealed that a key in achieving the best performance lies in the proper choice of the PS and TS coefficients. Additionally, it was shown that the optimized TSR protocol concedes the performance to the optimized PSR one while the IRR-based system always outperforms the latter. Finally, it was demonstrated that increasing the parameters α and/or μ of the α-μ results in reducing the ergodic OP.

Appendix A
Ergodic Outage Probability

For the sake of generality, the closed-form expressions for ergodic OP given by (34), (55) and (69) can be presented as

$$P_{\text{out}} = 1 - \frac{\alpha_1 \lambda_1^{\mu_1}}{2 \Gamma(\mu_1)} \sum_{n=0}^{\mu_2 - 1} \frac{\lambda_2^n}{n!} \left[1 - \frac{\gamma_{inc} \left(\mu_1, \frac{\psi_2 \gamma_{th}}{\psi_1} \right)}{\Gamma(\mu_1)} \right.$$
$$\left. - \frac{2 \Gamma \left(\mu_1 + n, \left(\frac{\psi_2 \gamma_{th}}{\psi_1 (\lambda_1 + \lambda_2)} \right)^{2/\alpha_1} \right)}{\alpha_1 (\lambda_1 + \lambda_2)^{\mu_1 + n}} \right], \quad (70)$$

where ψ_1, ψ_2 and ψ_3 are dependent on the EH protocol deployed; all of which are defined in Table I.

TABLE I. The parameters ψ_1, ψ_2 and ψ_3 for the TSR, PSR and IRR protocols.

	TSR	PSR	IRR
ψ_1	$2\eta\theta P_S$	$\rho(1-\rho)\theta P_S$	θP_S
ψ_2	$2\eta\theta d_1^m \sigma_R^2$	$\theta d_1^m \rho \left(\sigma_c^2 + (1-\rho)\sigma_a^2 \right)$	$\theta d_1^m \sigma_R^2$
ψ_3	$(1-\eta)d_1^m d_2^m \sigma_D^2$	$(1-\rho)d_1^m d_2^m \sigma_D^2$	$d_1^m d_2^m \sigma_D^2$

References

[1] D. Mishra, S. De, S. Jana, S. Basagni, K. Chowdhury, and W. Heinzelman, "Smart RF energy harvesting communications: challenges and opportunities," *IEEE Commun. Mag.*, vol. 53, no. 4, pp. 70–78, Apr. 2015.

[2] X. Zhou, R. Zhang, and C. K. Ho, "Wireless information and power transfer: Architecture design and rate-energy tradeoff," *IEEE Trans. Commun.*, vol. 61, pp. 4754–4767, Nov. 2013.

[3] S. Arzykulov, G. Nauryzbayev, T. A. Tsiftsis, and M. Abdallah, "On the Capacity of Wireless Powered Cognitive Relay Network with Interference Alignment," in *IEEE Global Commun. Conf. (Globecom)*, 1–6, Dec. 2017.

[4] K. Huang and E. Larsson, "Simultaneous information and power transfer for broadband wireless systems," *IEEE Trans. Signal Process.*, vol. 61, pp. 5972–5986, Dec. 2013.

[5] L. R. Varshney, "Transporting information and energy simultaneously," in *Proc. IEEE Int. Symp. Inf. Theory (ISIT)*, pp. 1612–1616, Jul. 2008.

[6] A. A. Nasir, X. Zhou, S. Durrani, and R. A. Kennedy, "Relaying protocols for wireless energy harvesting and information processing," *IEEE Trans. Wireless Commun.*, vol. 12, no. 7, pp. 3622–3636, Jul. 2013.

[7] G. Nauryzbayev, K. Rabie, M. Abdallah, and B. Adebisi, "Ergodic Capacity Analysis of Wireless Powered AF Relaying Systems over α-μ Fading Channels," in *IEEE Global Commun. Conf. (Globecom)*, 1–6, Dec. 2017.

[8] A. A. Nasir, X. Zhou, S. Durrani, and R. A. Kennedy, "Throughput and ergodic capacity of wireless energy harvesting based DF relaying network," in *Proc. IEEE Int. Conf. Commun. (ICC)*, pp. 4066–4071, Jun. 2014.

[9] K. M. Rabie, A. Salem, E. Alsusa, and M. S. Alouini, "Energy-harvesting in cooperative AF relaying networks over Log-normal fading channels," *IEEE Int. Conf. Commun. (ICC)*, pp. 1–7, May 2016.

[10] S. Arzykulov, G. Nauryzbayev, T. A. Tsiftsis, and M. Abdallah, "On the Performance of Wireless Powered Cognitive Relay Network with Interference Alignment," *IEEE Trans. Commun.*, May 2018, DOI: 10.1109/TCOMM.2018.2833104.

[11] G. Nauryzbayev, M. Abdallah and K. M. Rabie, "Outage Probability of Full-Duplex AF and DF Relaying Systems over $\alpha - \mu$ Channels," in *IEEE Vehicular Technology Conference (IEEE VTC2018-Fall)*, pp. 1-6, 2018.

[12] K. M. Rabie, B. Adebisi, and M. S. Alouini, "Wireless power transfer in cooperative DF relaying networks with Log-normal fading," in *Proc. IEEE Global Commun. Conf. (Globecom)*, pp. 1–6, Dec. 2016.

[13] A. Salem, K. Hamdi, and K. M. Rabie, "Physical layer security with RF energy harvesting in AF Multi-Antenna Relaying Networks," *IEEE Trans. Commun.*, vol. 64, no. 7, pp. 3025–3038, Jul. 2016.

[14] L. Zhao, X. Wang, and T. Riihonen, "Transmission Rate Optimization of Full-Duplex Relay Systems Powered by Wireless Energy Transfer," *IEEE Trans. Wireless Commun.*, vol. 16, no. 10, pp. 6438–6450, Oct. 2017.

[15] Y. Su, L. Jiang, and C. He, "Decode-and-forward relaying with full-duplex wireless information and power transfer," *IET Commun.*, vol. 11, no. 13, pp. 2110–2115, Oct. 2017.

[16] Z. Chang, X. Hou, X. Guo, T. Ristaniemi, and Z. Han, "Secure and Energy Efficient Resource Allocation for Wireless Power Enabled Full-/Half-Duplex Multiple-Antenna Relay Systems," *IEEE Trans. Veh. Technol.*, vol. 66, no. 12, pp. 11208–11219, Dec. 2017.

[17] J. Zhu, Y. Li, N. Wang, and W. Xu, "Wireless Information and Power Transfer in Secure Massive MIMO Downlink With Phase Noise," *IEEE Wireless Commun. Lett.*, vol. 6, no. 3, pp. 298–301, Jun. 2017.

[18] Z. Chang, Z. Wang, X. Guo, Z. Han, T. Ristaniemi, "Energy Efficient Resource Allocation for Wireless Power Transfer Enabled Massive MIMO System," in *Proc. IEEE Global Commun. Conf. (Globecom)*, pp. 1–7, Dec. 2016.

[19] I. Orikumhi, C. Y. Leow, and Z. Ding, "Wireless Information and Power Transfer in MIMO Virtual Full-Duplex Relaying System," *IEEE Trans. Veh. Technol.*, vol. 66, no. 12, pp. 11001–11010, Dec. 2017.

[20] Y. Ye, Y. Li, D. Wang, and G. Lu, "Power Splitting Protocol Design for the Cooperative NOMA with SWIPT," in *Proc. IEEE Int. Conf. Commun. (ICC)*, pp. 1–5, May 2017.

[21] Y. Xu, C. Shen, Z. Ding, X. Sun, S. Yan, G. Zhu, and Z. Zhong, "Joint Beamforming and Power-Splitting Control in Downlink Cooperative SWIPT NOMA Systems," *IEEE Trans. Signal Process.*, vol. 65, no. 18, pp. 4874–4886, Sep. 2017.

[22] W. Han, J. Ge, and J. Men, "Performance analysis for NOMA energy harvesting relaying networks with transmit antenna selection and maximal-ratio combining over Nakagami-m fading," *IET Commun.*, vol. 10, no. 18, pp. 2687–2693, Dec. 2016.

[23] O. Badarneh, "Energy Harvesting in α-μ Environment Under Different Relaying Protocols," *IEEE Wireless Commun. Lett.*, vol. 6, no. 6, pp. 814-817, Dec. 2017.

[24] A. M. Magableh and M. M. Matalgah, "Moment generating function of the generalized α-μ distribution with applications," *IEEE Commun. Lett.*, vol. 13, no. 6, pp. 411–413, Jun. 2009.

[25] S. Arzykulov, G. Nauryzbayev, and T. A. Tsiftsis, "Underlay cognitive relaying system over α-μ fading channels," *IEEE Commun. Lett.*, vol. 21, no. 1, pp. 216–219, Jan. 2017.

[26] I. S. Gradshteyn and I. M. Ryzhik, *Table of Integrals, Series, and Products*, San Diego, CA, USA: Academic Press, 2007.

[27] A. P. Prudnikov, Yu. A. Brychkov, and O. I. Marichev, *Integrals and Series, Vol. 3: More Special Functions*, Gordon and Breach, New York, 1990.

[28] M. D. Springer, *The algebra of random variables.* New York: Wiley, 1979.

[29] P. K. Mittal and K. C. Gupta, "An integral involving generalized function of two variables," *Proc. of the Indian Academy of Sciences - Section A,* vol. 75, pp. 117-123, Mar. 1972.

[30] A. Mathai, R. K. Saxena, and H. J. Haubold, *The H-Function theory and applications.* New York: Springer, 2010.

[31] S. Arzykulov, G. Nauryzbayev, T. A. Tsiftsis, and M. Abdallah, "Error Performance of Wireless Powered Cognitive Relay Networks with Interference Alignment," *in Proc. IEEE Int. Symp. Personal, Indoor, and Mobile Radio Commun. (PIMRC)*, 1–6, Oct. 2017.

[32] K. Hamdi, "A useful lemma for capacity analysis of fading interference channels," *IEEE Trans. Commun.*, vol. 58, no. 2, pp. 411–416, Feb. 2010.

[33] M. D. Yacoub, "The α-μ Distribution: A Physical Fading Model for the Stacy Distribution channels," *IEEE Trans. Veh. Technol.*, vol. 56, no. 1, pp. 27–34, Jan. 2007.